# Novel Paromamine Derivatives Exploring Shallow-Groove Recognition of Ribosomal-Decoding-Site RNA

Klaus B. Simonsen,*[a] Benjamin K. Ayida,[a] Dionisios Vourloumis,[a] Masayuki Takahashi,[a] Geoffrey C. Winters,[a] Sofia Barluenga,[a] Seema Qamar,[b] Sarah Shandrick,[b] Qiang Zhao,[b] and Thomas Hermann*[b]

*Natural aminoglycoside antibiotics recognize an internal loop of bacterial ribosomal-decoding-site RNA by binding to the deep groove of the RNA structure. We have designed, synthesized, and tested RNA-targeted paromamine derivatives that exploit additional interactions on the shallow groove face of the decoding-site RNA. An in vitro transcription – translation assay of a series of 6′-derivatives showed the 6′-position to be very sensitive to substitution. This result suggests that the group at the 6′-position plays a pivotal role in RNA target recognition.*

**KEYWORDS:**

aminoglycosides · antibiotics · drug design · medicinal chemistry · RNA recognition

The bacterial ribosome is a key target for antibiotics, which recognize predominantly the ribosomal RNA (rRNA) components.[1, 2] Aminoglycoside antibiotics[3] such as paromomycin (**2**, Figure 1 A) target the decoding-site RNA (Figure 1 B) within the 30S ribosomal subunit, and thereby interfere with translation fidelity,[4] an effect that ultimately leads to bacterial cell death. Molecular recognition of the decoding-site internal-loop RNA by natural aminoglycosides[1, 2, 5–8] and synthetic derivatives[9–12] has been studied by biochemical, biophysical, and theoretical methods. Three-dimensional structures of the decoding-site RNA and the whole 30S ribosomal subunit complexed with aminoglycosides have been determined recently.[2, 6, 7] These results pave the way for structure-based rational design of novel antibiotics[13] that may overcome bacterial resistance to natural aminoglycosides[14] and demonstrate superior pharmacological profiles. For the time being, aminoglycosides provide the best validated paradigm in RNA target recognition,[15] which justifies the challenging undertaking to prepare rationally designed derivatives in order to elucidate the structure – activity relationships of RNA-directed ligands.

Herein, we describe the design, synthesis, and preliminary testing of paromamine (**1**) 6′- and 4′-derivatives based on a scaffold common to the biologically active natural aminoglycosides. Structural data from X-ray crystallography[2, 7] along with our own molecular modeling studies[16] suggested that extension at the 6′-position of paromamine might allow for additional hydrogen-bond interactions with the decoding-site RNA (Figure 1 C). The N1 atom of adenine 1408 and the O2 atom of cytosine 1409 in the RNA shallow groove may form direct interactions with hydrogen bond donors at the paromamine 6′-position, or water-mediated contacts with hydrogen-bond acceptors. In the RNA complex the 4′-hydroxy group of paromamine is directed towards the flipped-out adenine residues 1492 and 1493, which play a key role in mRNA decoding during translation.[2, 3] It has been suggested that binding of aminoglycosides to the decoding site displaces A1492 and A1493 from the deep groove of the internal-loop RNA, which compensates in part for the energetic cost of the conformational changes induced by cognate tRNA binding.[2] Thus, in the presence of aminoglycoside bound at the decoding site, incorporation of noncognate tRNAs is facilitated and this effect leads to decreased translational fidelity. Molecular modeling[16] suggests that larger aromatic groups extending from the paromamine 4′-position, directed out of the RNA shallow groove, might be able to contribute interactions with the flipped-out A1492 and A1493 residues. Modifications, both at the 6′- and 4′-positions, were aimed at increasing the potential of the paromamine derivatives to bind to the decoding-site RNA and stabilize the flipped-out conformation of the unpaired adenine residues in order to enhance the efficacy of the ligands to interfere with bacterial decoding-site function.

We synthesized paromamine derivatives with diverse functional groups at the 6′-position and aromatic residues at the 4′-

[a] *Dr. K. B. Simonsen, Dr. B. K. Ayida, Dr. D. Vourloumis, M. Takahashi, G. C. Winters, Dr. S. Barluenga*
*Department of Medicinal Chemistry*
*Anadys Pharmaceuticals, Inc.*
*9050 Camino Santa Fe, San Diego, CA 92121 (USA)*
*Fax:(+ 1) 858-527-1539*
*E-mail: ksimonsen@anadyspharma.com*

[b] *Dr. T. Hermann, Dr. S. Qamar, S. Shandrick, Dr. Q. Zhao*
*Departments of RNA Biochemistry and Computational Chemistry & Structure*
*Anadys Pharmaceuticals, Inc.*
*9050 Camino Santa Fe, San Diego, CA 92121 (USA)*
*Fax:(+ 1) 858-527-1539*
*E-mail: thermann@anadyspharma.com*

  1439-4227/02/03/12 $ 20.00+.50/0 

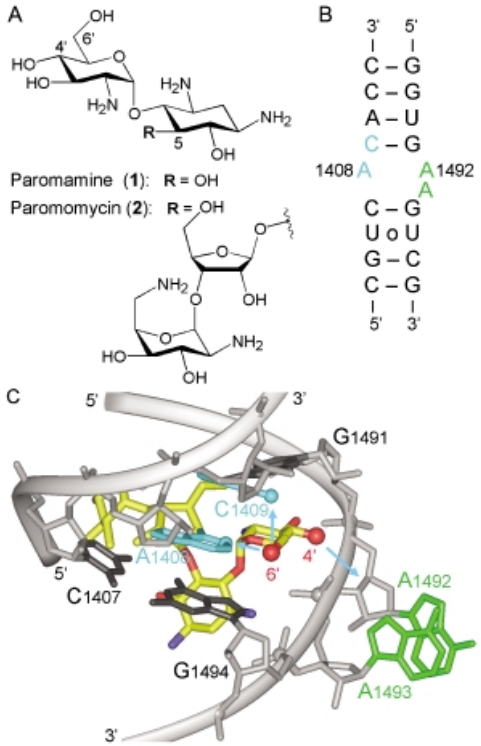


***Figure 1.*** *A) Paromamine (**1**), the conserved core scaffold of naturally occuring aminoglycoside antibiotics such as paromomycin (**2**), which binds specifically to the decoding site of bacterial rRNA. B) Secondary structure of the bacterial decoding-site rRNA. C) Three-dimensional structure of paromomycin (**2**; yellow) bound to the bacterial decoding-site rRNA.[2] Oxygen and nitrogen atoms in the paromamine core are colored red and blue, respectively. The flipped-out adenine residues A1492 and A1493 are shown in green. The bases A1408 and C1409, which are in proximity to the paromomycin 6′ hydroxy group, are colored cyan. Arrows indicate potential interactions of substituents attached at the 4′- and 6′-positions of paromamine.*

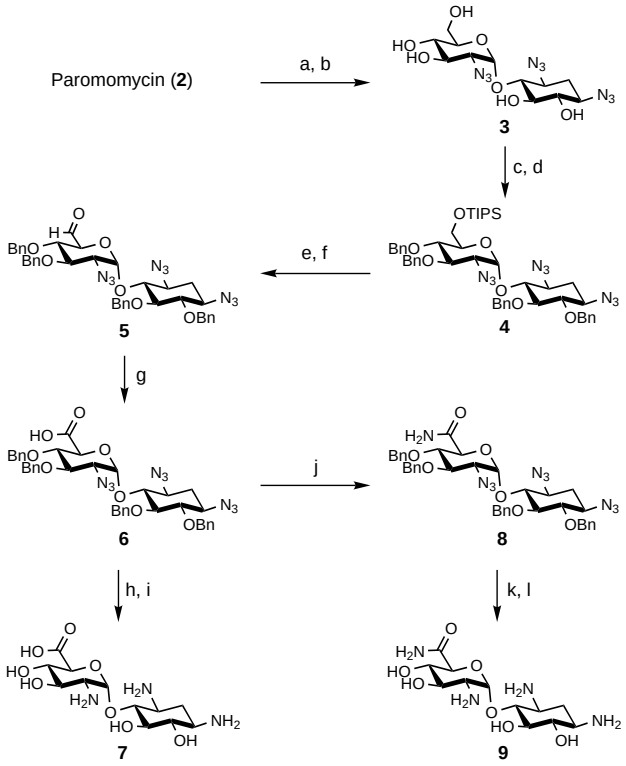


***Scheme 1.*** *Reagents and conditions: a) concd HCl, MeOH (0.1 M), 6 h, reflux, 99%; b) $TfN_3$ (0.5 M in $CH_2Cl_2$, 4.5 equiv), $CuSO_4 \cdot 5H_2O$ (0.15 equiv), $Et_3N$ (15.0 equiv, MeOH/$H_2O$ (9:1, 0.1 M), 16 h, 23 °C, 88%; c) TIPSCl (2.0 equiv), 4-DMAP (3.0 equiv), DMF (0.1 M), 23 °C, 85%; d) NaH (8.0 equiv), BnBr (6.0 equiv), DMF (0.2 M), 4 h, 0 → 23 °C, 80%; e) TBAF (1.0 M in THF, 2.0 equiv), THF (0.1 M), 3 h, 0 → 23 °C, 73%; f) Dess – Martin periodinane (2.0 equiv), $CH_2Cl_2$ (0.05 M), 3 h, 0 °C, 70%; g) $NaClO_2$ (2.0 equiv), $NaH_2PO_4$ (3.0 equiv), 2-methyl-2-butene (2 M in THF, 10.0 equiv), tBuOH/$H_2O$ (2:1), THF, 3 h, 23 °C, 95%; h) $Me_3P$ (1 M in THF, 4.5 equiv), 0.1 M NaOH/THF (1:9), 4 h, 23 °C; i) $Pd(OH)_2$ (0.05 equiv), $H_2$, AcOH/$H_2O$ (1:1), 20 h, 23 °C, 60% (two steps); j) $(COCl)_2$ (2.0 equiv), DMF (2.0 equiv), $CH_2Cl_2$, 30 min, − 20 → 0 °C; then acid **6** (1.0 equiv), 10 min, − 20 → 0 °C; then $NH_3$ (7 N in MeOH, 10.0 equiv), 1 h, 0 → 23 °C, 54%; k) $Me_3P$ (1 M in THF, 4.5 equiv), 0.1 M NaOH/THF (1:9), 4 h, 23 °C; l) $Pd(OH)_2$ (0.05 equiv), $H_2$, AcOH/$H_2O$ (1:1), 20 h, 23 °C, 98% (two steps). Tf = trifluoromethanesulfonyl; TIPS = triisopropylsilyl; 4-DMAP = 4-dimethylaminopyridine; DMF = N,N-dimethylformamide; TBAF = tetra-n-butylammonium fluoride; THF = tetrahydrofuran.*

position then tested their binding to the decoding-site RNA and their efficacy as inhibitors of bacterial in vitro translation. Additional paromamine derivatives were synthesized by selective methylation of hydroxy groups in either the glucosamine moiety or in the 2-deoxystreptamine (2-DOS) unit or in both rings. These compounds, along with derivatives that had all amino groups transformed into ureas or methyl-ureas, were tested to further explore the importance of polar substituents on the periphery of paromamine.

The syntheses of the 6′-analogues of paromamine are summarized in Schemes 1 – 3. Commercially available paromomycin (**2**) was hydrolyzed under mild acidic conditions (0.1 M HCl/MeOH) to paromamine[17] (**1**), which was converted into the triazide **3** by the action of triflic azide in the presence of $CuSO_4$.[18] The 6′ hydroxy group was then selectively protected with TIPSCl in the presence of 4-DMAP. The remaining hydroxy groups were benzylated to produce compound **4**. Subsequent silyl deprotection with TBAF followed by Dess – Martin periodinane oxidation provided the 6′-aldehyde **5** in good overall yields. The six-step synthetic sequence of compound **5**, which constitutes a late common intermediate, was easily carried out on gram scale. The final steps in the synthesis of the 6′-carboxylic acid **7** and amide **9** of paromamine are outlined in Scheme 1.

Aldehyde **5** was oxidized to the corresponding carboxylic acid **6** by using $NaClO_2/NaH_2PO_4$. Although deprotection of the benzyl groups and reduction of the azides could be carried out simultaneously, the final deprotection/reduction sequence was conducted in a two-step deprotection protocol, as reported by Wong and co-workers.[10] Hence, treatment of **6** with $Me_3P$ in THF under mild basic conditions provided the corresponding triamine, which was hydrogenated in the presence of a catalytic amount of $Pd(OH)_2$ to provide **7** in 50% yield after chromatography. Treatment of the carboxylic acid **6** with the Vilsmeier complex generated from oxalyl chloride and DMF (1:1) provided the corresponding acyl chloride, which was converted into amide **8** upon treatment with ammonia in methanol and deprotected by the same two-step protocol as above to furnish **9** in 53% overall yield.

The syntheses of the one-carbon homologated amide **12** and aldehyde **13** are illustrated in Scheme 2. Several synthetic

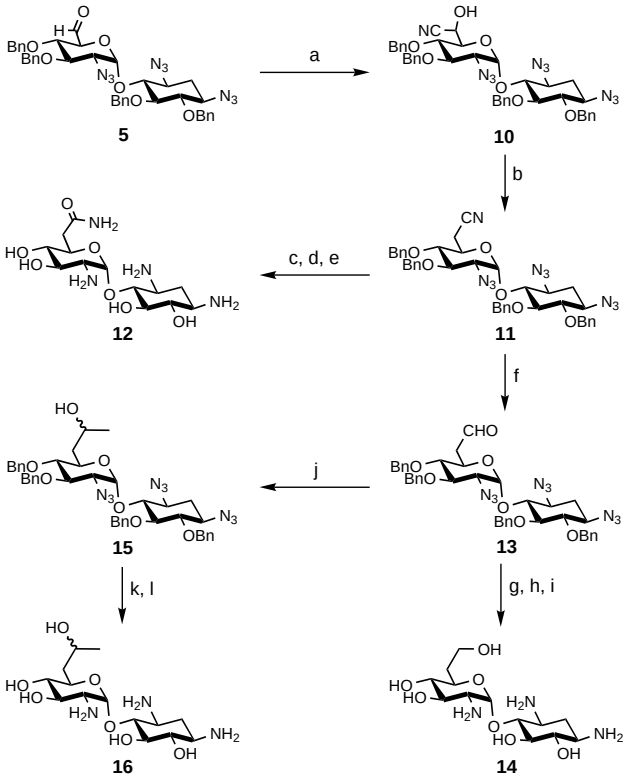


*Scheme 2. Reagents and conditions: a) $Et_2AlCN$ (1.0 M in toluene, 2.0 equiv), toluene (0.1 M), 3 h, −10 °C; b) 4-DMAP (0.2 equiv), $Im_2CS$ (1.2 equiv), $CH_2Cl_2$, (0.05 M), 40 min, 23 °C; then AIBN (0.2 equiv), n$Bu_3SnH$ (5.0 equiv), hν, 1 h, 23 °C, 55% (three steps); c) n$Bu_4NHSO_4$ (0.2 equiv) $H_2O_2$/2 M NaOH/$CH_2Cl_2$ (1:1:1), 48 h, 23 °C, 35%; d) $Me_3P$ (1 M in THF, 4.5 equiv), 0.1 M NaOH/THF (1:9), 4 h, 23 °C; e) $Pd(OH)_2$ (0.05 equiv) $H_2$, AcOH/$H_2O$ (1:1), 20 h, 23 °C, 87% (two steps); f) DIBAL-H (1 M in $CH_2Cl_2$, 2.5 equiv), $CH_2Cl_2$ (0.1 M), 2 h, 0 °C; then 1 M HCl, 15 min, 23 °C, 90%; g) $NaBH_4$ (1.0 equiv), THF (0.05 M), 2 h, 23 °C, 68%; h) $Me_3P$ (1 M in THF, 4.5 equiv), 0.1 M NaOH/THF (1:9), 4 h, 23 °C; i) $Pd(OH)_2$ (0.05 equiv), $H_2$, AcOH/$H_2O$ (1:1), 20 h, 23 °C, 79% (two steps); j) MeMgBr (1.4 M in THF, 4.0 equiv), THF (0.1 M), 3 h, −78 °C, 35%; k) $Me_3P$ (1 M in THF, 4.5 equiv), 0.1 M NaOH/THF (1:9), 4 h, 23 °C; l) $Pd(OH)_2$ (0.05 equiv), $H_2$, AcOH/$H_2O$ (1:1), 20 h, 23 °C, 92% (two steps). Im = imidazole; AIBN = 2,2′-azobisisobutyronitrile; DIBAL-H = diisobutylaluminum hydride.*

protocols, which included Wittig homologation of aldehyde **5** and Arndt–Eistert synthesis from acid **6**, proved unsuccessful for the desired homologation. Eventually, the one-carbon homologation protocol developed by Nicolaou et al. gave the desired nitrile **11**.[19] Treatment of aldehyde **5** with $Et_2AlCN$ in toluene provided cyanohydrin **10**, which was converted without purification into nitrile **11** upon sequential treatment with thiocarbonyl diimidazole, *n*$Bu_3SnH$/AIBN, and light. Mild basic hydration[20] of the cyano functionality in **11** was achieved under phase-transfer conditions to provide the homologated amide **12** in 17% overall yield after deprotection.

The importance of hydrogen bond donors in the vicinity of the 6′-position was investigated with the derivatives shown in Schemes 2 and 3. 6′-Homoparomamine **14** was prepared from nitrile **11** in four steps (see Table 1 for analytical data for **14** and selected other compounds). DIBAL-H reduction at 0 °C followed by acidic work-up afforded aldehyde **13**, which was further reduced to the corresponding alcohol with $NaBH_4$ and finally

***Table 1.** Characteristic analytical data of selected compounds.*

**6′-Homoparomamine 14**: $^1$H NMR (400 MHz, $D_2O$): $\delta = 5.55$ (d, $J = 4.0$ Hz, 1H), 3.85–3.20 (m, 11H), 2.42 (dt, $J = 12.4$, 4.0 Hz, 1H), 2.04 (m, 1H), 1.80 (q, $J = 12.8$ Hz, 1H), 1.59 (m, 1H) ppm; $^{13}$C NMR (100 MHz, $D_2O$): $\delta = 97.2$, 80.1, 75.2, 73.3, 72.6, 69.7, 69.2, 54.4, 50.4, 49.9, 48.9, 32.8, 28.4 ppm; MS (ESI): *m/z*: calcd for $C_{13}H_{28}N_3O_7$ $[M+H]^+$: 338.19; found: 338 (100%).

**6′-Methyl-paromamine 18**: inseparable 3:2 mixture of diastereomers (unassigned); major: $^1$H NMR (400 MHz, $D_2O$): $\delta = 5.78$ (d, $J = 4.0$ Hz, 1H), 4.25 (qd, $J = 6.8$, 2.0 Hz, 1H), 4.00–3.35 (m, 9H), 2.56 (dt, $J = 12.4$, 4.4 Hz, 1H), 1.95 (q, $J = 12.4$ Hz, 1H), 1.34 (d, $J = 6.8$, 3H) ppm; $^{13}$C NMR (100 MHz, $D_2O$): $\delta = 97.3$, 80.1, 75.9, 75.1, 72.5, 69.8, 69.2, 64.9, 54.1, 49.9, 49.1, 28.3, 19.0 ppm; MS (ESI): *m/z*: calcd for $C_{13}H_{28}N_3O_7$ $[M+H]^+$: 338.19; found: 338 (100%); minor: $^1$H NMR (400 MHz, $D_2O$): $\delta = 5.62$ (d, $J = 4.0$ Hz, 1H), 4.29 (qd, $J = 6.8$, 2.0 Hz, 1H), 4.00–3.35 (m, 9H), 2.27 (dt, $J = 12.4$, 4.4 Hz, 1H), 1.62 (q, $J = 12.4$ Hz, 1H), 1.26 (d, $J = 6.8$, 3H) ppm; $^{13}$C NMR (100 MHz, $D_2O$): $\delta = 97.9$, 82.0, 75.5, 74.7, 72.5, 70.3, 69.7, 65.5, 54.4, 49.8, 49.3, 28.5, 14.7 ppm; MS (ESI): *m/z*: calcd for $C_{13}H_{28}N_3O_7$ $[M+H]^+$: 338.19; found: 338 (100%).

**4,5-Dimethoxy-paromamine 26**: $^1$H NMR (400 MHz, $D_2O$): $\delta = 5.64$ (d, $J = 3.6$ Hz, 1H), 4.03 (t, $J = 10.0$ Hz, 1H), 4.08–3.42 (m, 10H), 3.70 (s, 3H), 3.67 (s, 3H), 2.54 (dt, $J = 12.4$, 4.0 Hz, 1H), 1.91 (q, $J = 12.4$ Hz, 1H) ppm; $^{13}$C NMR (100 MHz, $D_2O$): $\delta = 95.7$, 83.5, 82.3, 76.9, 74.2, 69.4, 69.0, 60.6, 60.5, 59.6, 54.0, 49.1, 49.0, 28.2 ppm; MS (ESI): *m/z* calcd for $C_{14}H_{30}N_3O_7$ $[M+H]^+$: 352.21; found: 352 (100%).

**Urea 29**: $^1$H NMR (400 MHz, $D_2O$): $\delta = 5.24$ (br s, 1H), 3.80–3.34 (m, 10H), 3.22 (t, $J = 10.0$ Hz, 1H), 1.97 (br dt, $J = 13.2$, 3.2 Hz, 1H), 1.35 (q, $J = 12.4$ Hz) ppm; $^{13}$C NMR (100 MHz, $D_2O$): $\delta = 161.4$ (br, 2C), 160.7, 98.7, 81.0, 77.1, 75.4, 72.2, 71.6, 69.9, 60.6, 54.7 (br), 50.4 (br), 48.9 (br), 34.5 ppm; MS (ESI): *m/z* calcd for $C_{15}H_{29}N_6O_{10}$ $[M+H]^+$: 453.19; found: 453 (100%).

**Benzotriazole 40**: $^1$H NMR (400 MHz, $D_2O$): $\delta = 8.32$ (s, 1H), 7.90 (d, $J = 8.8$ Hz, 1H), 7.75 (d, $J = 8.8$ Hz, 1H), 5.47 (d, $J = 4.0$ Hz, 1H), 4.15 (m, 1H), 4.07 (dd, $J = 9.2$, 13.6 Hz, 1H), 3.84–3.64 (m, 5H), 3.59 (t, $J = 9.6$ Hz, 1H), 3.52 (t, $J = 10.0$ Hz, 1H), 3.21 (m, 2H), 2.32 (dt, $J = 12.8$, 4.0 Hz, 1H), 1.63 (q, $J = 12.8$ Hz, 1H), 1.59 ppm; MS (ESI): *m/z* calcd for $C_{19}H_{29}N_6O_8$ $[M+H]^+$: 469.20; found: 469 (100%).

deprotected to provide **14**. Addition of MeMgBr to aldehyde **13** followed by standard deprotection produced the methyl analogue **16** in good yield as a 3:1 mixture of diastereomers (unassigned). Preparation of the 6′-methyl paromamine **18** and the diol analogue **21** was achieved as shown in Scheme 3. Treatment of aldehyde **5** with MeMgBr produced the desired alcohol **17** as a 3:2 mixture of diastereomers (unassigned), which furnished **18** upon deprotection. Wittig homologation of **5** with $Ph_3P{=}CH_2$ afforded terminal alkene **19**, which was dihydroxylated with $OsO_4$ and NMO in the presence of a catalytic amount of quinuclidine. The resulting diol **20** was isolated as a 3:1 mixture of diastereomers (unassigned) and was subsequently deprotected to give the desired diol **21**.

The role of the different amino and hydroxy groups in the interaction of paromamine with RNA was investigated next. Three compounds (**22**, **24**, and **26**) were synthesized (Scheme 4) in which the hydrogen bond donor ability of the hydroxy functionalities was hampered by selective methylation. The 6′-TIPS-protected paromamine **3a** was treated with MeI, deprotected with TBAF, and finally reduced under Staudinger conditions to produce **22**. The 3′,4′-dimethoxy paromamine analogue **24** was prepared from **3a** in five steps. Treatment of **3a** with 2,2-dimethoxypropane in the presence of *p*-TsOH afforded monoacetonide **23** in 65% yield. This compound was methylated upon exposure to MeI and NaH. Deprotection of the TIPS group under standard conditions (TBAF), followed by hydrolysis

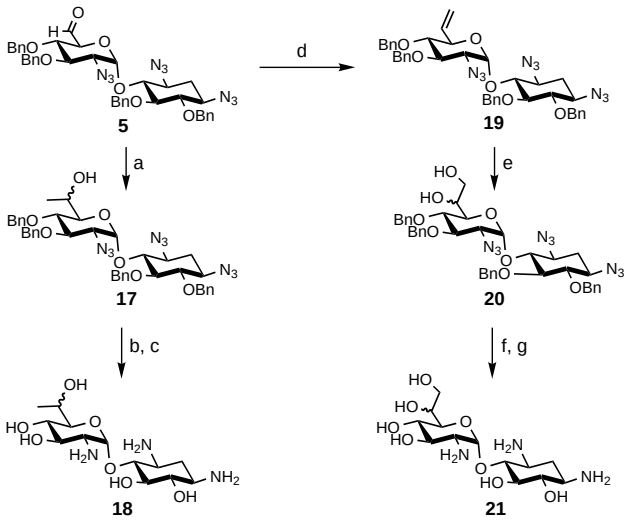

***Scheme 3.*** *Reagents and conditions: a) MeMgBr (1.4 M in THF, 2.0 equiv), THF, 3 h, −78 °C, 45 %; b) $Me_3P$ (1 M in THF, 4.5 equiv), 0.1 M NaOH/THF (1:9), 4 h, 23 °C; c) $Pd(OH)_2$ (0.05 equiv), $H_2$, AcOH/$H_2O$ (1:1), 20 h, 23 °C, 83 % (two steps); d) methyltriphenylphosphonium bromide (2.5 equiv), THF (0.1 M), 0 °C, nBuLi (1.6 M in hexane, 2.0 equiv), 30 min; then* ***5*** *(1.0 equiv) in THF, 1 h, 0 → 23 °C, 59 %; e) NMO (2.0 equiv), quinuclidine (0.1 equiv), $OsO_4$ (2 wt % in tBuOH, cat), acetone/$H_2O$ (15:1), 23 °C, 70 %; f) $Me_3P$ (1 M in THF, 4.5 equiv), 0.1 M NaOH/THF (1:9), 4 h, 23 °C; g) $Pd(OH)_2$ (0.05 equiv) $H_2$, AcOH/$H_2O$ (1:1), 20 h, 23 °C, 94 % (two steps). NMO = 4-methylmorpholine* N*-oxide.*

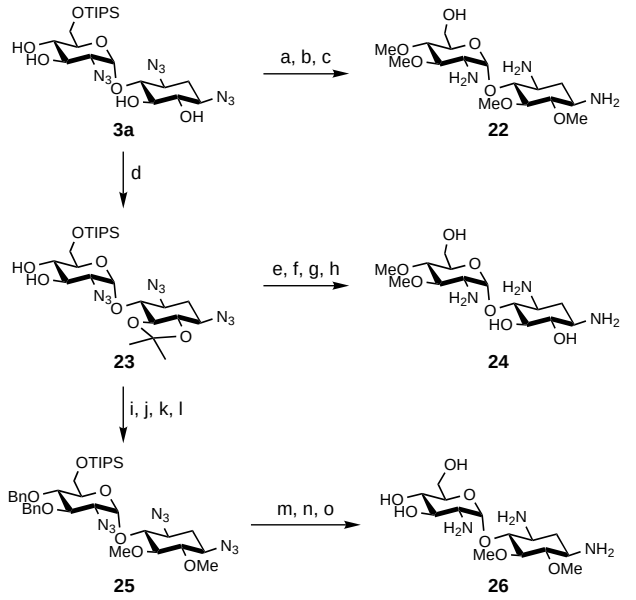

***Scheme 4.*** *Reagents and conditions: a) NaH (6.0 equiv), MeI (8.0 equiv), DMF (0.1 M), 18 h, 0 → 23 °C, 82 %; b) TBAF (1.0 M in THF, 1.3 equiv), THF (0.04 M) 1.5 h, 0 → 23 °C, 99 %; c) $Me_3P$ (1 M in THF, 4.0 equiv), 0.1 M NaOH/THF (1:9), 3.5 h, 23 °C, quantitative; d) 2,2-dimethoxypropane (20.0 equiv),* p*-TsOH (0.1 equiv), acetone (0.07 M), 5 h, 0 → 23 °C, 65 %; e) NaH (4.0 equiv), MeI (6.0 equiv), DMF (0.1 M), 2 h, 0 → 23 °C, 81 %; f) TBAF (1.0 M in THF, 1.5 equiv), THF (0.07 M), 1.5 h, 0 → 23 °C, 76 %; g) 1 M HCl/THF (1:1), 24 h, 23 °C, 91 %; h) $Me_3P$ (1 M in THF, 4.0 equiv), 0.1 M NaOH/THF (1:9), 3.5 h, 23 °C, quantitative; i) NaH (4.0 equiv), BnBr (6.0 equiv), DMF (0.10 M), 2 h, 0 → 23 °C, 62 %; j) 1 M HCl/THF (1:1), 24 h, 23 °C, 67 %; k) TIPSCl (1.5 equiv), 4-DMAP (4.0 equiv), DMF (0.05M), 2 h, 0 → 23 °C, 64 %; l) NaH (4.0 equiv), MeI (6.0 equiv), DMF (0.04 M), 1.5 h, 0 → 23 °C, 80 %; m) TBAF (1.0 M in THF, 1.3 equiv), THF (0.03 M), 2 h, 0 → 23 °C, 88 %; n) $Me_3P$ (1 M in THF, 4.0 equiv), 0.1 M NaOH/THF (1:9), 5 h, 23 °C; o) $Pd(OH)_2$ (0.05 equiv), $H_2$, AcOH/$H_2O$ (1:1), 20 h, 23 °C, quantitative (both steps). Ts = toluenesulfonyl.*

(1 M HCl) of the acetonide and Staudinger reduction of the azides furnished **24** in 56 % overall yield. The synthesis of **26** required an additional seven steps from the acetonide **23**. The remaining hydroxy groups in **23** were benzylated by using BnBr in DMF. Subsequently, the acetonide was cleaved under standard acidic hydrolysis (1 M HCl), which unfortunately resulted in simultaneous removal of the silicon protecting group. Hence, the primary alcohol was reprotected with TIPSCl in the presence of 4-DMAP and the corresponding diol was methylated (MeI/NaH) to produce **25** in 22 % overall yield from **23**. Finally, desilylation of the TIPS group with TBAF and Staudinger reduction of the azides followed by catalytic hydrogenolysis of the benzyl groups afforded **26** in 88 % overall yield.

The syntheses of two urea analogues of paromamine (**29**, **30**) are shown in Scheme 5. Triazide **3** was perbenzylated and further reduced under Staudinger conditions to provide the corresponding triamine **27**. The amino groups were conveniently

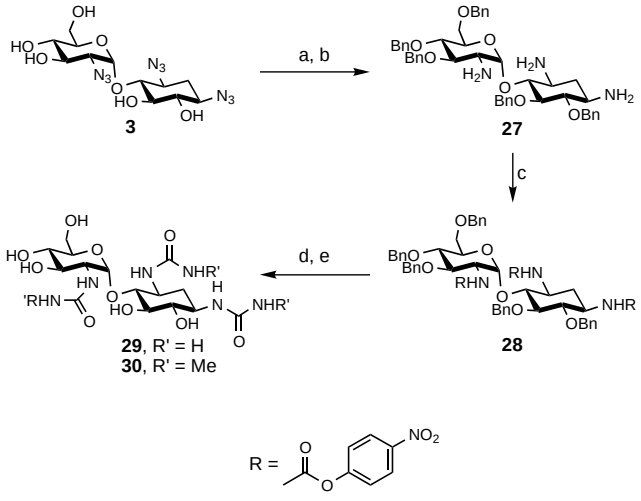

***Scheme 5.*** *Reagents and conditions: a) NaH (10.0 equiv), BnBr (8.0 equiv), DMF (0.2 M), 18 h, 0 → 23 °C, 65 %; b) $Me_3P$ (1 M in THF, 4.5 equiv), 0.1 M NaOH/THF (1:9), 4 h, 23 °C, 80 %; c) bis(4-nitrophenyl)carbonate (3.5 equiv), $CH_2Cl_2$ (0.05 M), 18 h, 23 °C, 55 %; d) $NH_3$ (2 M in MeOH, 6.0 equiv, 18 h) or $MeNH_2$ (40 wt % in $H_2O$, 6.0 equiv, 10 min), $CH_2Cl_2$ (0.01 M), 0 °C; e) $Pd(OH)_2$ (0.05 equiv), $H_2$, AcOH/$H_2O$ (1:1), 20 h, 23 °C, 60 % for* ***29*** *(two steps) and 59 % for* ***30*** *(two steps).*

converted into the corresponding ureas by following the procedure developed by Izdedski and Pawlak.[21] Hence, treatment of **27** with bis(4-nitrophenyl)carbonate afforded the activated triscarbamate **28**, which was further converted into the corresponding ureas by addition of $NH_3$ or $MeNH_2$ and finally deprotected to afford compounds **29** and **30**, respectively.

Four amide analogues **37** – **40** were synthesized as depicted in Scheme 6 in order to explore the space that extends out from the 4′-position of paromamine for potential interactions with the adenine residues 1492 and 1493 of the decoding-site RNA. Initially, the amides were introduced onto the carbohydrate scaffold from the reduced form of **31** and the appropriate acyl chlorides prior to coupling. Unfourtunately, the amide functionality in the 4′-position disrupted coupling with **34**, probably as a

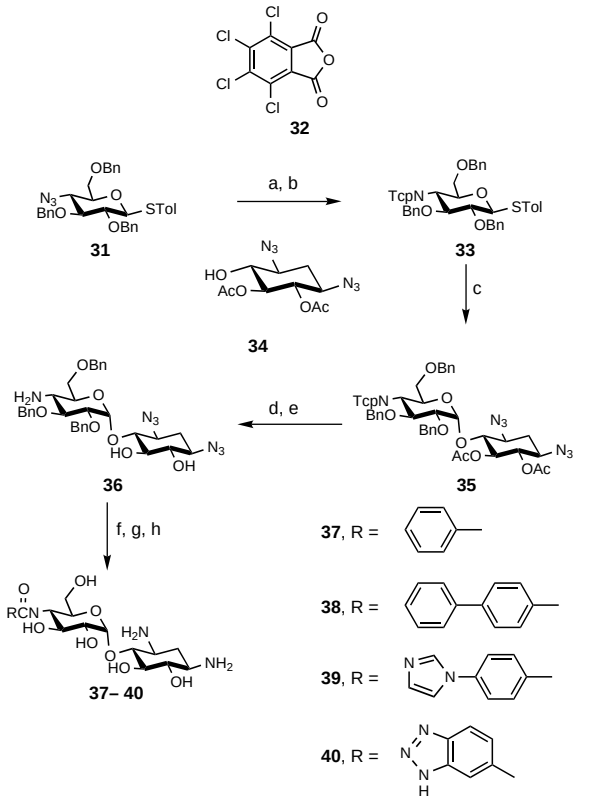


***Scheme 6.*** *Reagents and conditions: a) $Me_3P$ (1 M in THF, 1.5 equiv), 0.1 M NaOH/THF (1:9), 4 h, 23 °C; b)* ***32*** *(1.2 equiv), pyridine (0.09 M), 18 h, 23 °C; then $Ac_2O$ (10.0 equiv), 1 h, 23 °C, 93%; c)* ***33*** *(1.0 equiv),* ***34*** *(1.2 equiv), NIS (2.2 equiv), MS (4 Å), TfOH (0.28 equiv), $Et_2O/CH_2Cl_2$ (3:2, 0.01 M), 1 h, −20 °C, 74%; d) ethylenediamine (5.0 equiv), EtOH (0.03 M), 20 h, 50 °C; e) $K_2CO_3$ (6.0 equiv), MeOH (0.03 M), 2 h, 23 °C, 98% (two steps); f) $(COCl)_2$ (1.5 equiv), DMF (1.5 equiv), 30 min, −20 → 0 °C; then acids (1.5 equiv), 10 min,* ***36*** *(1.0 equiv), $iPr_2NEt$ (1.4 equiv), 1.5 h, 0 → 23 °C, 70 – 86%; g) $Me_3P$ (1 M in THF, 3.0 equiv), 0.1 M NaOH/THF (1:9), 4 h, 23 °C; h) $Pd(OH)_2$ (0.05 equiv), $H_2$, AcOH/$H_2O$ (1:1), 20 h, 23 °C, quantitative (two steps). MS = molecular sieves. NIS =* N*-iodosuccinimide.*

result of an intramolecular attack of the amide carbonyl group on the generated oxocarbenium ion,[22] which would result in a stable seven-membered *N*-aryl imidate. The presence of azido groups in glycosyl acceptor **34** dictated a different protecting strategy for the amine functionality in **31.** The azido group was converted into the corresponding amine under Staudinger conditions and further protected as the tetrachlorophthalimide (Tcp) **33**. Treatment of the amine with tetrachlorophthalic anhydride **32** in pyridine provided the open benzoic acid intermediate, which was dehydrated to **33** upon treatment with acetic anhydride. 2-Deoxystreptamine acceptor **34**[10] was glycosylated with donor **33** in the presence of NIS and triflic acid, providing pseudo-disaccharide **35**. The Tcp protecting group was removed under standard conditions (ethylenediamine) and the crude product was further deprotected with $K_2CO_3$/MeOH to provide the amino diol **36**. Treatment of **36** with the appropriate acyl chloride in the presence of $Et_3N$ and further deprotection as above furnished amides **37** – **40** in good overall yields.

The biological activity of the compounds was evaluated in a coupled in vitro transcription – translation assay with firefly luciferase as a reporter (Table 2). Binding to the decoding-site RNA target was confirmed for compounds that had an $IC_{50}$ value below 200 μM in the translation assay by a fluorescence-based RNA affinity assay.[23] Among the paromamine derivatives that had modified hydrogen bond donor functionalities, as in the methoxy compounds **22**, **24**, and **26**, or the ureas **29** and **30**, only derivative **26**, which is methylated at the 2-DOS hydroxy groups, retained biological activity, albeit at a drastically reduced level. This observation is in line with the fact that many natural aminoglycoside antibiotics possess additional sugar moieties at the O5 and O6 positions. Simplified nonglycosidic substituents at the O5 hydroxy group of 2-DOS have been reported to result in loss of biological activity,[9, 10, 24] whereas some synthetic modifications at the O6 hydroxy group seem to retain antibacterial potency.[12]

None of the synthesized 6′- or 4′-derivatives showed superior activity to paromamine in the translation assay. The $IC_{50}$ values of

***Table 2.*** *Structure – activity relationships for paromamine derivatives.*

| | Compound | $R^1$ | $R^2$ | $IC_{50}$ [mM][a] |
|---|---|---|---|---|
| 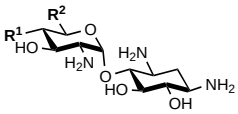 | **1** | OH | $CH_2OH$ | 3.9[b] |
| | **7** | OH | COOH | 620 |
| | **9** | OH | C(=O)$NH_2$ | > 1000 |
| | **12** | OH | $CH_2$C(=O)$NH_2$ | 380 |
| | **14** | OH | $CH_2CH_2OH$ | 170[b] |
| | **16** | OH | $CH_2$CH(∼OH)$CH_3$ | 97[b] |
| | **18** | OH | CH(∼OH)$CH_3$ | 23[b] |
| | **21** | OH | CH(∼OH)$CH_2OH$ | 24[b] |
| | **37** | C(=O)-phenyl | $CH_2OH$ | > 1000 |
| | **38** | C(=O)-4-biphenyl | $CH_2OH$ | 380 |
| | **40** | C(=O)-6-benzotriazole | $CH_2OH$ | 450 |
| 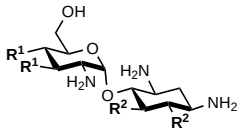 | **22** | $OCH_3$ | $OCH_3$ | > 1000 |
| | **24** | $OCH_3$ | OH | > 1000 |
| | **26** | OH | $OCH_3$ | 250 |
| 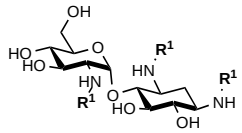 | **29** | C(=O)$NH_2$ | - | > 1000 |
| | **30** | C(=O)$NHCH_3$ | - | > 000 |

[a] The coupled in vitro transcription – translation assay was carried out in a 384-well plate. The test compound was incubated with bacterial S30 extract (Promega) followed by a mixture that contained nucleotide triphosphates, amino acids, and pBEST*luc* plasmid DNA (Promega) encoding the luciferase reporter. Plates were incubated at 25 °C for 20 min. After cooling on ice, SteadyGlow luciferin substrate (Promega) was added, followed by incubation for 15 min at room temperature. Light emission from the plates was recorded with a TopCount (Perkin Elmer) luminescence counter. Each compound was tested in a dose-response fashion at concentrations ranging from 1 mm to 100 nm. $IC_{50}$ values were determined from light unit versus log(*c*) plots by fitting to a variable slope dose-response equation. Six replicate experiments were run per concentration. An excellent signal-to-noise ratio was obtained in the assay, attested by *Z*′ values[25] in the range of 0.60 – 0.70 per plate. To rule out the possibility that active compounds were inhibitors of the bacterial RNA polymerase or firefly luciferase reporter enzyme, all compounds were counter-screened against polymerase and luciferase. None of the paromamine derivatives inhibited either polymerase or luciferase. [b] Binding to the decoding-site-RNA target was confirmed by a fluorescence-based RNA affinity assay.[23]

the 4′-substituted paromamines were at least 100-fold higher than that of the parent compound. Interestingly, the activity increased with the size of the aromatic substituent; 4′-biphenyl paromamine **38** displayed the lowest $IC_{50}$ value. Even small deviations from the primary alcohol substitution at the 6′-position, such as an additional methyl group as in **18**, reduced the potency at least sixfold. Introduction of a second exocyclic hydroxy group, as in the diol **21**, did not restore biological activity. Similarly, potency was lost after removal of the hydroxy group further from the pyranose by insertion of an additional methylene group, as in **14** and **16**. Replacement of the 6′-hydroxy group by hydrogen-bond acceptor groups or mixed acceptor – donors, as in the carboxylic acid **7** and the amides **9** and **12**, led to dramatic reduction of activity.

In summary, the observed structure – activity relationships for the paromamine 6′-derivatives reveal an exquisite sensitivity of the 6′-position towards substitution, which emphasizes the pivotal role of the group in this position in RNA target recognition. This role is confirmed by a recently published high-quality crystal structure of paromomycin bound to a decoding-site RNA construct.[7] This structure shows the 6′ hydroxy group of paromamine involved in key hydrogen-bond interactions with the RNA that align the pyranose ring with the adenine 1408 base in a striking Watson – Crick base pair fashion.[7] The interactions between the paromamine pyranose ring and A1408 have been suggested to contribute significantly to aminoglycoside specificity toward the bacterial decoding site.[7]

*This work was supported in part by a National Institutes of Health grant to T.H.*


[1] a) D. Moazed, H. F. Noller, *Nature* **1987**, *327*, 389 – 394; b) J. Woodcock, D. Moazed, M. Cannon, J. Davies, H. F. Noller, *EMBO J.* **1991**, *10*, 3099 – 3103; c) P. Purohit, S. Stern, *Nature* **1994**, *370*, 659 – 662.

[2] a) A. P. Carter, W. M. Clemons, D. E. Brodersen, R. J. Morgan-Warren, B. T. Wimberly, V. Ramakrishnan, *Nature* **2000**, *407*, 340 – 348; b) D. E. Brodersen, W. M. Clemons, A. P. Carter, R. J. Morgan-Warren, B. T. Wimberly, V. Ramakrishnan, *Cell* **2000**, *103*, 1143 – 1154; c) J. M. Ogle, D. E. Bordersen, W. M. Clemons, M. J. Tarry, A. P. Carter, V. Ramakrishnan, *Science* **2001**, *292*, 897 – 902.

[3] G. D. Wright, A. M. Berghuis, S. Mobashery in *Resolving the Antibiotic Paradox: Progress in Understanding Drug Resistance and Development of New Antibiotics* (Eds.: B. P Rosen, S. Mobashery), Plenum, New York, **1998**, pp. 27 – 69.

[4] a) V. Ramakrishnan, *Cell* **2002**, *108*, 557 – 572; b) R. Schroeder, C. Waldsich, H. Wank, *EMBO J.* **2000**, *19*, 1 – 9.

[5] C.-H. Wong, M. Hendrix, E. S. Priestley, W. A. Greenberg, *Chem. Biol.* **1998**, *5*, 397 – 406.

[6] a) M. I. Recht, D. Fourmy, S. C. Blanchard, K. D. Dahlquist, J. D. Puglisi, *J. Mol. Biol.* **1996**, *262*, 421 – 436; b) D. Fourmy, M. I. Recht, S. C. Blanchard, J. D. Puglisi, *Science* **1996**, *274*, 1367 – 1371; c) D. Fourmy, S. Yoshizawa, J. D. Puglisi, *J. Mol. Biol.* **1998**, *277*, 333 – 345; d) D. Fourmy, M. I. Recht, J. D. Puglisi, *J. Mol. Biol.* **1998**, *277*, 347 – 362.

[7] Q. Vicens, E. Westhof, *Structure* **2001**, *9*, 647 – 658.

[8] C. Ma, N. A. Baker, S. Joseph, J. A. McCammon, *J. Am. Chem. Soc.* **2002**, *124*, 1438 – 1442.

[9] P. Alper, M. Hendrix, P. Sears, C.-H. Wong, *J. Am. Chem. Soc.* **1998**, *120*, 1965 – 1978.

[10] W. A. Greenberg, E. S. Priestley, P. S. Sears, P. B. Alper, C. Rosenbohm, M. Hendrix, S.-C. Hung, C.-H. Wong, *J. Am. Chem. Soc.* **1999**, *121*, 6527 – 6541.

[11] S. Hanessian, M. Tremblay, A. Kornienko, N. Moitessier, *Tetrahedron* **2001**, *57*, 3255 – 3265.

[12] J. Haddad, L. P. Kotra, B. Llano-Sotelo, C. Kim, E. F. Azucena, M. Liu, S. B. Vakulenko, C. S. Chow, S. Mobashery, *J. Am. Chem. Soc.* **2002**, *124*, 3229 – 3237.

[13] a) T. Hermann, *Angew. Chem.* **2000**, *112*, 1962 – 1979; *Angew. Chem. Int. Ed.* **2000**, *39*, 1890 – 1904; b) T. Hermann, E. Westhof, *Comb. Chem. High Throughput Screening* **2000**, *3*, 219 – 234; c) J. Gallego, G. Varani, *Acc. Chem. Res.* **2001**, *34*, 836 – 843.

[14] L. P. Kotra, J. Haddad, S. Mobashery, *Antimicrob. Agents Chemother.* **2000**, *44*, 3249 – 3256.

[15] a) Y. Tor, T. Hermann, E. Westhof, *Chem. Biol.* **1998**, *5*, R277 – R283; b) K. Michael, Y. Tor, *Chem. Eur. J.* **1998**, *4*, 2091 – 2098; c) T. Hermann, E. Westhof, *Biopolymers* **1999**, *48*, 155 – 165; d) S. J. Suchek, Y.-K. Shue, *Curr. Opin. Drug Discovery Dev.* **2001**, *4*, 462 – 470.

[16] Molecular modeling was performed by using published atom coordinates of the 30S ribosomal-subunit – aminoglycoside complexes[2] and high-resolution crystal structures of a synthetic 35-nucleotide RNA construct, which contained the bacterial decoding-site internal loop (Q. Zhao, T. Hermann, unpublished results). The conformational space available to the 6′ hydroxy group of paromamine docked to the decoding-site RNA was explored by using the Insight/Discover (Accelrys) program and the AMBER force field following established protocols: T. Hermann, E. Westhof, *J. Med Chem.* **1999**, *42*, 1250 – 1261.

[17] T. H. Haskell, J. C. French, Q. R. Bartz, *J. Am. Chem. Soc.* **1959**, *81*, 3480 – 3481.

[18] P. B. Alper, S.-C. Hung, C.-H. Wong, *Tetrahedron Lett.* **1996**, *37*, 6029 – 6032.

[19] K. C. Nicolaou, G. Vassilikogiannakis, R. Kranich, P. S. Baran, Y.-L. Zhong, S. Natarajan, *Org. Lett.* **2000**, *2*, 1895 – 1898.

[20] S. Cacchi, D. Misiti, F. La Torre, *Synthesis* **1980**, 243 – 244.

[21] J. Izdedski, D. Pawlak, *Synthesis* **1989**, 423 – 425.

[22] For compounds with 1,2-, 1,3-, and 1,6-cyclic imidate on the carbohydrate scaffold, see, for example: a) A. Vasella, C. Witzig, *Helv. Chim. Acta.* **1995**, *78*, 1971 – 1982; b) R. G. Dushin, S. J. Danishefsky, *J. Am. Chem. Soc.* **1992**, *114*, 3471 – 3475; c) S. Allemann, J.-L. Reymand, P. Vogel, *Helv. Chim. Acta.* **1990**, *73*, 674 – 689.

[23] S. Shandrick, S. Qamar, T. Hermann, **2002**, submitted.

[24] S. Hanessian, M. Tremblay, A. Kornienko, N. Moitessier, *Tetrahedron* **2001**, *57*, 3255 – 3265.

[25] J.-H. Zhang, T. D. Y. Chung, K. R. Oldenburg, *J. Biomol. Screening* **1999**, *2*, 67 – 73.


Received: June 18, 2002 [F 440]